Synthesis of graphene quantum dots/TiO_2 nanocomposites and its application for detection of Chromium(VI) ions by photoluminescence spectroscopy

Tran Thi Bich Quyen[1*], Nguyen Thanh Kha[1], Nguyen Nguyen Hoang Dang Khoa[1], Ngo Nguyen Tra My[1], Doan Van Hong Thien[1], Luong Huynh Vu Thanh[1]

[1]Department of Chemical Engineering, College of Technology, Can Tho University, 3/2 Street, Ninh Kieu District, Can Tho City, Vietnam

***Corresponding Author:** Tran Thi Bich Quyen; E-mail: ttbquyen@ctu.edu.vn; Can Tho University

Abstracts

In this study, Graphene Quantum Dots (GQDs)/TiO_2 nanocomposites were successfully synthesized by a simple, easy to implement method with a fast reaction time (30 min) and low reaction temperature (60^{o}C). In particular, graphene quantum dots (GQDs) nanoparticles are obtained by green and environmentally friendly synthetic method using abundant and naturally available raw materials from rice starch and under supporting of microwave irradiation at power 900 W for 10 min. The synthesized GQDs were determined the morphology by Transmission electron microscope (TEM) with average particle size ~8-15 nm. In addition, the synthesized GQDs were successful combined with TiO_2 nanoparticles (TiO_2 NPs) to form GQDs/TiO_2 nanocomposites with highly optical property and photocatalytic activity. These GQDs/TiO_2 nanocomposites synthesized were also analyzed their characterizations, morphologies and compositions by: UV-vis, FTIR, XRD, TEM and EDX. Results showed that GQDs/TiO_2 nanocomposites were spherical in shape, with average particle size of ~10-25 nm; and their components obtained including: C (41.36%); O (54.08%); and Ti (4.56%), respectively. Moreover, these GQDs/TiO_2 nanocomposites were also applied in the detection of Chromium(VI) ions with lowest limit of detection (LOD) for Chromium(VI) ions concentration being ~0.1 μM and in the wide detection range from 0.01 M to 0.1 μM by photoluminescence spectroscopy (PL). Therefore, the obtained GQDs/TiO_2 nanocomposites have potential to be developed as photocatalyst materials applications in many fields such as sensors, biosensors, sensors, biomedical, optoelectronics, etc.

Keywords: *graphene quantum dots/TiO_2 nanocomposites (GQDs/TiO_2 NCPs); photocatalyst; photoluminescence spectroscopy (PL); graphene quantum dots (GQDs); rice starch; detection of Chromium(VI) ions.*

I. Introduction

For many years, nanomaterials have shown significantly distinctive properties as compared to bulk materials. Graphene quantum dots (GQDs) is a new material and has the potential to replace semiconductor quantum dots (QDs) in several applications such as biomedical [1, 2], sensors [3, 4], solar cells [5], and Spintronics [6]… Legacy graphene quantum dots (GQDs) some of the most prominent properties of graphene but in contrast to large versions of graphene experimental and theoretical studies of GQDs have low toxicity [7], biocompatibility [8], negligible environmental impact [9, 10] and high optical stability easily dispersed in a variety of solvents.

The combination of organic–inorganic nanoparticles composition or hybrids have attracted much interest due to their current and potential applications as they can combine useful chemical, optical and mechanical characteristics [11, 12] in recent years.

Titanium dioxide nanoparticles, especially the anatase form of TiO_2 that has more oxygen vacancies than the rutile phase, has a high photocatalytic efficiency under UV light [13]. Titania-based materials are very attractive due to their inherent high refractive index and UV absorbing properties. Besides, because of its impressive properties such as chemical stability, good optical transparency, low cost, and non-toxicity [14], Titanium dioxide nanoparticles (TiO_2 NPs) have broadly used as a photocatalyst for solar energy conversion [15], a building material [16], a bleaching agent [17], and gas sensors for monitoring air pollution [18]. One drawback that limit Titania's practical application is its high bandgap energy (~3-3.2 eV) which requires the use of a radiation in the ultraviolet region to produce electron and hole pairs. Recent reports have been shown that the electron-hole pair on TiO_2 tends to be easy to recombine and has a relatively low adsorption capacity [19, 20]. Therefore, several solutions have been implemented to reduce the bandgap energy in the visible light region as well as reduce the re-pairing of electrons and holes. A promising candidate can be combined with TiO_2 NPs is GQDs because of its luminescent and eco-friendly ability. Indeed, this new material not only has a smaller band energy than TiO_2 NPs but also can be biodegradable.

As known, graphene quantum dots (GQDs) successful combined with TiO_2 nanoparticles (TiO_2 NPs) using simply and rapidly, low-cost, and environment-friendly synthetic method at low temperature has not yet reported previously. Herein, we report an eco-friendly and economical method to prepare graphene quantum dots (GQDs) from natural scource being rice starch and ascorbic acid (AA) under supporting of microwave irradiation at power of 900 W for 10 min. In addition, TiO_2 nanoparticles (TiO_2 NPs) were modified on the surface by GQDs nanoparticles using simple method with rapid reaction time of 30 min at 60^{o}C. Furthermore, GQDs/TiO_2

nanocomposites have also applied in the detection of Chromium(VI) ions by photoluminescence spectroscopy (PL). Results shown that the good adsorption capability of GQDs/TiO_2 nanocomposites (GQDs/TiO_2 NCPs) in promoting direct electron transfer and greatly intensitive enhancement capability of GQDs/TiO_2 NCPs for detection of Chromium(VI) ions on the PL signal. Thus, GQDs/TiO_2 NCPs are potential and promising novel nanomaterials applications in photocatalysis, bio-sensor, sensor in chemical/electrochemical, environment and optical transparency, etc.

II. Materials and Methods

a. Materials

Ascorbic acid ($C_6H_8O_6$, 99,7%); Titanium Butoxide (($Ti(OBu)_4$, 99%); Ethylene Glycol ($C_2H_4(OH)_2$; 99%); Ammonium Chlorite (NH_4Cl; 99%) and Sulfuric acid (H_2SO_4, 98%) were bought from Sigma-Aldrich. Rice starch was purchased at Can Tho City. All solutions were prepared with deionized water from a MilliQ system.

b. Syntheis of graphene quantum dots (GQDs)

0.15 g of rice starch and 6 mL of ascorbic acid were stirred with 19 mL of deioned water (DI H_2O) for 15 min. Then, prepared precursor solution were heated at a power level of 900 W under supporting of microwave irradiation for 8, 10, 12 and 14 min, respectively. Subsequently, dark brown solid was allowed to cool down at room temperature and added into 25 mL of DI H_2O. The mixture was sonicated for 30 min to have a brown solution. Pre-product was centrifuged at 4000 rpm for 20 min to remove the insoluble solids. Finally, synthesized GQDs was stored at 2°C for using next step.

c . Preparation of TiO_2 nanoparticles

0.75 mL of $Ti(OBu)_4$ was dropped slowly into 5 mL $C_2H_4(OH)_2$ during 20 min. Those were stirred homogeneously by heating a magnetic stirrer to form a gel. After that, the gel was poured into a 100 mL solution of 3.5 g NH_4Cl and dissolved carefully in H_2SO_4 0.1 M. The reaction was carried out and stirred at 90°C for 1 h. The product was collected by centrifugated, washed with DI H_2O for several times and stored in 10 mL of DI H_2O for further characterization.

d. Synthesis of graphene quantum dots/TiO_2 nanocomposites

Prepared TiO_2 NPs (0.5, 1, 1.5 and 2 mL) was added into a solution of GQDs (5 mL) and distilled water (5mL). The above solution mixture was stirred at 60°C for 30 min. And then, these

$GQDs/TiO_2$ nanocomposites were separated by centrifugation and washed with DI H_2O several times to obtain $GQDs/TiO_2$ nanocomposites purity. The obtained $GQDs/TiO_2$ nanocomposites ($GQDs/TiO_2$ NCPs) was also re-dissolved in 10 mL of DI H_2O to prepare for using as photocatalyst materials.

e. Preparation of graphene quantum dots/TiO_2 nanocomposites ($GQDs/TiO_2$ NCPs) catalyst for detection of Chromium(VI) ions

2 mL of Chromium(VI) salt solution with different concentrations sequential: (0,1 μM, 1 μM, 500 μM, 5 mM, 10 mM) was added into 2 mL of $GQDs/TiO_2$ nanocomposites solution. After that, the mixture was stirred vigorous in 5 min at room temperature.

f. Characterization of synthesized $GQDs/TiO_2$ nanocomposites

The $GQDs/TiO_2$ NPs synthesis was observed by recording the absorbance spectra between 200 and 900 nm on the UV-vis spectrophotometer (Thermo Scientific Evolution 60S UV-Vis spectrophotometer, USA). X-ray diffraction (XRD) was performed on a D8-Advance machine (Bruker, Germany) in the 2θ range of 10°-80°. The Fourier transform infrared (FT-IR) spectra were obtained by Perkin Elmer Frontier MIR/NIR (Perkin Elmer, USA) was conducted in KBr pellet at room temperature in the range of 4000-400 cm^{-1}. Transmission electron microscopy (TEM) characterization was performed on a Jem1010 device (Joel Company, Japan). Chemical properties and constituent components were analyzed via Energy-dispersive X-ray spectroscopy (EDX H-7593, Horiba, England). Photoluminescence spectra (PL) was recorded at 350 nm using FluoroMax-4 spectrofluorometer (Horiba Jobin Yvon, France).

III. Results and Discussion

3.1 Characterization and morphology of the $GQDs/TiO_2$ nanocomposites

In Figure 1A shows the UV-vis spectra result of GQDs. As it is clear, GQDs absorption spectra shows a clear absorption in the band from 300 to 310 nm due to $n \rightarrow \pi^*$ transition of the C=O [21]. Specially, after 10 min of microwave treament, obtained GQDs sample has the highest maximum absorption intensity compared to another samples. When reaction time protracted, the excitation energy for the system was increased which made the carbonization process occurred faster, lead to the amount/concentration of GQDs synthesized be also increased. But when reaction time was too long, the formation of GQDs nanoparticles in solution decreased gradually due to the excessive of carbonization and oxidation. In addition, the UV-vis spectra in Figure 1B indicated that, depending on the volume of TiO_2 nanoparticles (TiO_2 NPs) solution, appreciable changes will occur in GQDs/TiO_2 nanocomposites. Specificlly, the peak from 300 to 310 nm has changed to 295 nm and the bandgap of GQDs/TiO_2 (3.1 eV) is lower than that of pure TiO_2 (3.2 eV) sample. GQDs not only reduced the band energy of TiO_2 NPs, it also increased the visible light absorption of TiO_2. Besides, optical properties of GQDs/TiO_2 nanocomposites are also significantly improved when compared to that of pure TiO_2 NPs.

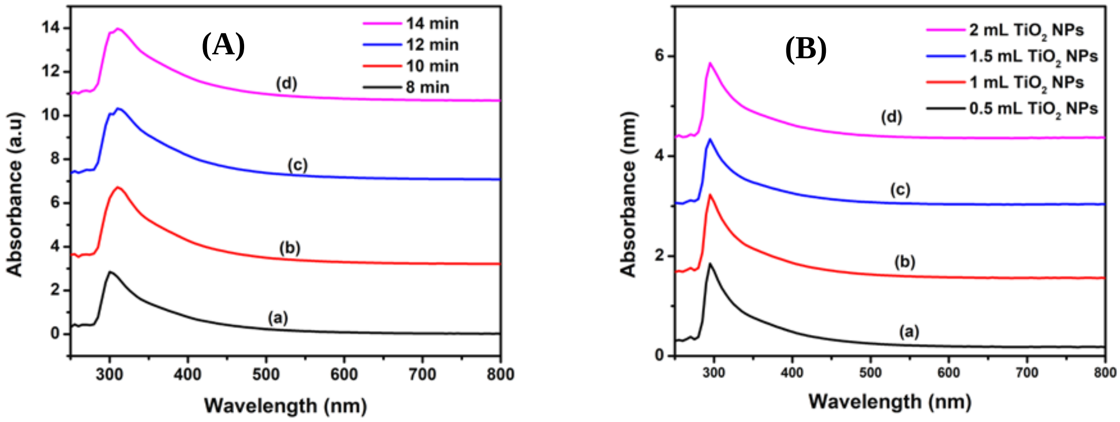

Figure 1. UV-vis spectras of (A) graphene quantum dots (GQDs) under supporting of microwave irradiation with various reaction times of (a) 8 min, (b) 10 min, (c) 12 min, and (d) 14 min; and (B) GQDs/TiO_2 nanocomposites (GQDs/TiO_2 NCPs) with different mounts of TiO_2 NPs solution; respectively.

Figure 2 shows the FTIR spectra of the samples of interest. Fristly, absorption band of the GQDs sample (Figure 2(b)) at 3420 cm^{-1} was attributed to the hydroxyl (-OH) groups (stretching mode) [13]. Additionally, the GQDs showed absorption of stretching vibration –O-C=O at 2309 cm^{-1} and stretching vibration of –C-O-C in the range at 1244 cm^{-1} [14]. The peak around 1693 cm^{-1} corresponding to C=O bonds. The transformation of chemical groups in GQDs when adding TiO_2 NPs was shown in Figure 2(a). The broad absorption band around 3449 cm^{-1} was enhanced in the presence of TiO_2 NPs (perhaps because $Ti(OH)_4$ enhanced the stretch vibration of the –OH group). In addition, peaks at 605 cm^{-1} and 1660 cm^{-1} were attributed the vibrations of the Ti-O group and the bending of the molecules water was adsorbed respectively in TiO_2 NPs surface [22]. The absorption peak at 2928 cm^{-1} originates from the stretching vibration of the C-H bond. The peaks around 2928 cm^{-1}, 1194 cm^{-1} and 1050 cm^{-1} originates from the stretching vibration of the C-H bonds, C-O-C in epoxide bonds and the combination of Ti-O-Ti and Ti-O-C oscillations [22]. Meantime, the characteristic adsorption peak at 785 cm^{-1} corresponding to the Ti-O-Ti bond vibration of TiO_2 appeared [23]. These indicated that TiO_2 in GQDs/TiO_2 nanocomposites was in situ formed.

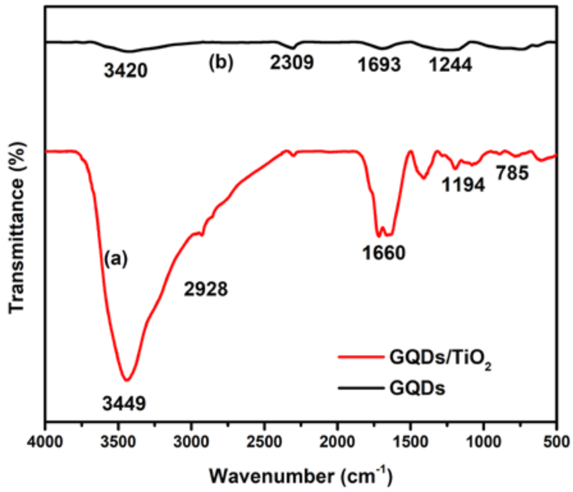

Figure 2. FTIR spectra of: (a) GQDs/TiO_2 nanocomposites and (b) GQDs, respectively.

As shown in Figure 3, the result X-ray diffraction (XRD) of samples were obtained corresponding to the GQDs and GQDs/TiO_2 nanocomposites. A typical, XRD profile of the prepared GQDs was shown in Figure 3(b). As could been seen, there is a amorphous diffraction peak at an angle of $2\theta = 26°$ corresponding to the (002) plane of graphene suggesting that rice starch produced a graphene structure in the synthesized GQDs [24]. Meanwhile, the XRD result of GQDs/TiO_2 nanocomposites sample-shown in Figure 3(a), there are 5 clear peaks with 2θ values respective being 25.3°; 38.6°; 48.0°; 53.9° and 62°, corresponding to the crystal planes of (110), (111), (200), (220) and (311) of anatase TiO_2 crystaline (JCPDS No. 21-1272) [24, 25]. The diffraction peak of GQDs is not observed in the GQDs/TiO_2 nanocomposites may be due to the relatively low diffraction intensity of GQDs and the amorphous peak (002) of GQDs was affected by the (101) plane diffraction peak of TiO_2. Therefore, GQDs have been successfully attached/combined to the surface of TiO_2 NPs to form GQDs/TiO_2 nanocomposites [26].

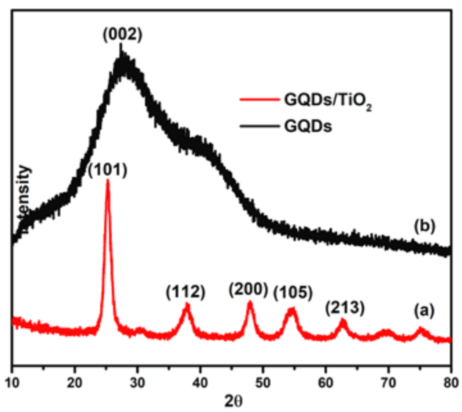

Figure 3. X-ray diffraction (XRD) of: (a) GQDs/TiO_2 nanocomposites and (b) GQDs, respectively.

The morphology of the GQDs/TiO_2 nanocomposites was studied by transmission electron microscopy (TEM). As shown in Figure 4, the GQDs/TiO_2 nanoparticles - at optimal conditions consisting of 5 mL of GQDs solution and 1 mL of TiO_2 NPs solution, are uniformly distributed. After observation of TEM image, it demonstrated that the mainly shape of the synthesized GQDs/TiO_2 nanocomposites have the spherical structure with an average particle size ~10-25 nm.

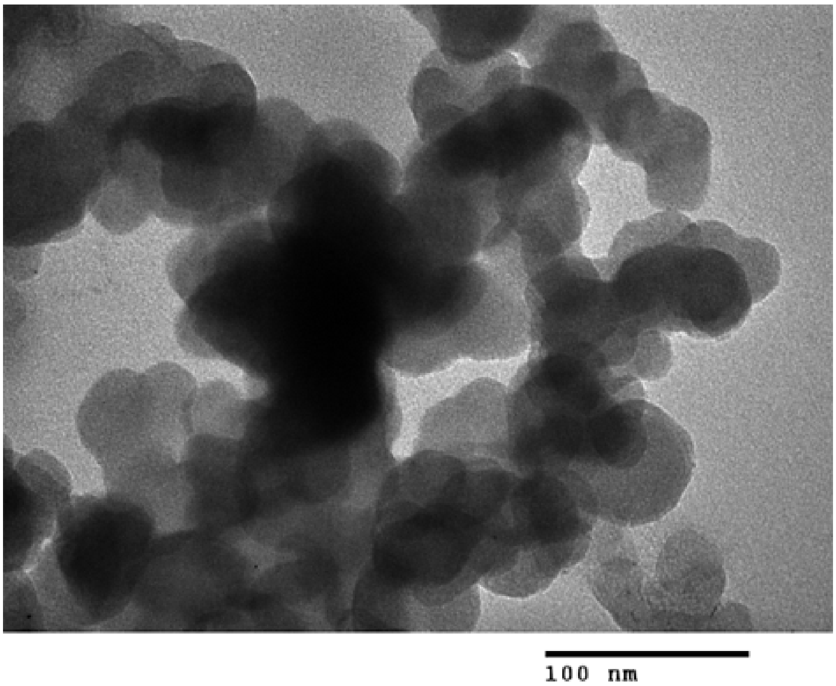

Figure 4. TEM image of GQDs/TiO_2 nanocomposites.

EDX analysis was performed to check the percent (%) component of all elements of the synthesized GQDs/TiO_2 nanocomposites specimen. Figure 5 shows that the GQDs/TiO_2 nanocomposites correspond to the composition/mass of elements including: C (41, 36%); O (54.08%); Ti (4.56%) and no other peak for any other element has been found. Oxygen content in sample is quite large because the GQDs/TiO_2 nanocomposite contains several characteristic function groups which contain oxygen element such as: O-H; C=O; -COO-; -C-O; -C-O-C; -SO_3^{2-}; Ti–O;.. This is consistent with the FTIR result as shown in Figure 2. In this manner, the GQDs/TiO_2 nanomaterials carry many polar functional groups containing oxygen, which can predict the good solubility of this material in polar solvents such as water, etc.

International Journal of Scientific Engineering and Applied Science (IJSEAS) – Volume-7, Issue-6, June 2021
ISSN: 2395-3470
www.ijseas.com

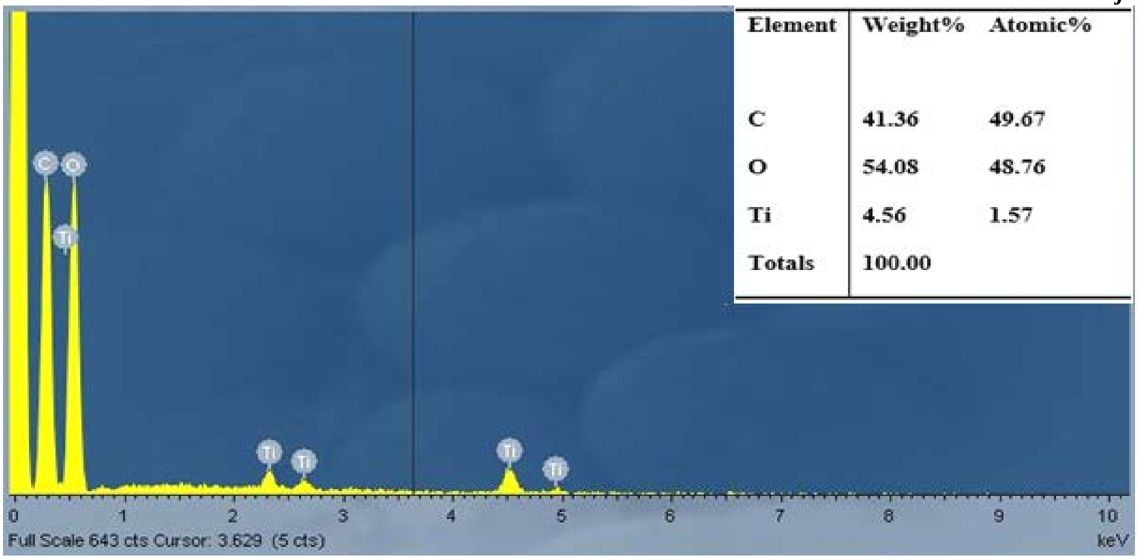

Figure 5. EDX spectra of $GQDs/TiO_2$ nanocomposites.

3.2 Application of $GQDs/TiO_2$ nanocomposites material for Chromium(VI) (Cr^{6+}) ions detection by photoluminescence (PL) spectroscopy

Depending on the different concentrations of Cr^{6+} ions, the $GQDs/TiO_2$ nanocomposites samples have different interactions leading to significant changes in the fluorescence emission spectroscopy (PL) result - shown in Figure 6. The comparison chart of the PL emission intensity/signal (Figure 7) shows that the percentage (%) of the emission signal difference between pure $GQDs/TiO_2$ nanocomposite (without the presence of Cr^{6+} ions) and other samples within the presence of various Cr^{6+} ions concentrations, respectively. The obtained results show that, under an excitation wavelength of 350 nm (UV), the PL spectra tend to be emitted the same corresponding luminescence wavelength at 436 nm (visible light). The maximum emission peak of $GQDs/TiO_2$ nanocomposites samples does not have significantly shift. When changing the concentration of Cr^{6+} ions, the emission signal intensity on the PL spectra of $GQDs/TiO_2$ nanocomposites are significantly difference – respective as shown in Figures 6 and 7. The samples have higher concentrations of Cr^{6+} ions, the luminescence signal intensity on the PL spectrum tends to decrease gradually. In particular, for solutions with Cr^{6+} ions at a concentration of 10 mM, the luminescence intensity of $GQDs/TiO_2$ nanocomposites ($GQDs/TiO_2$ NCPs) decreased sharply to 96.65%, which shows that Cr^{6+} ions have the potential fluorescence "quenching" of $GQDs/TiO_2$ nanomaterial. Based on this result, it can be confirmed that $GQDs/TiO_2$ nanocomposites has a high capability to detect the presence of Cr^{6+} ions as well as heavy other metal ions. The limit of detection (LOD) of Cr^{6+} ions is obtained at extremely low concentration ~0.1 μM and within the wide detection range corresponding to the concentration of Cr^{6+} ions from 0.1 μM to 10 mM. Thus, the synthesized

$GQDs/TiO_2$ nanocomposites can be potential and promising photocatalytic materials for practical applications in many fields such as photocatalysis (environmental treatment), electrochemical sensor catalyst, biomedical sensor, energy (solar battery), etc.

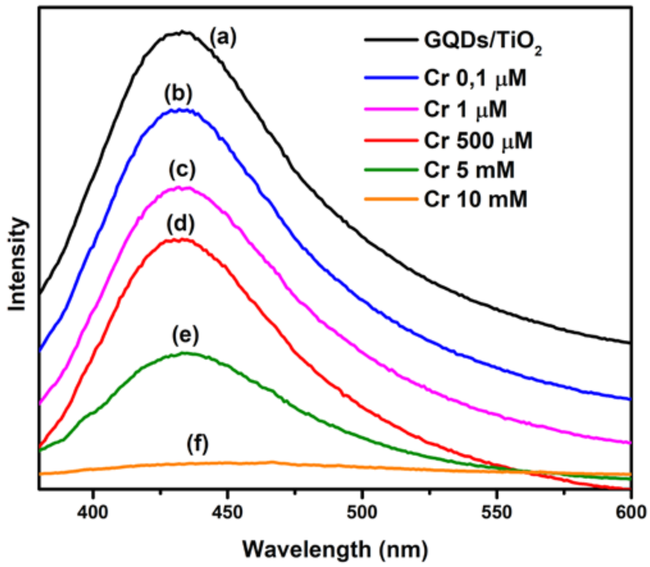

Figure 6. Photoluminescence (PL) spectroscopy of $GQDs/TiO_2$ nanocomposites with different concentrations of Chromium(VI) ions respective: (a) 0 M, (b) 0.1 μM, (c) 1 μM, (d) 500 μM, (e) 5 mM, and (f) 10 mM with the excitation wavelength at 350 nm.

Table 1. Obtained signal intensity at emission wavelength of 436 nm on the PL spectroscopy of $GQDs/TiO_2$ nanocomposites samples with different concentrations of Cr^{6+} ions respective with excitation wavelength of 350 nm.

Samples	**Intensity (I)**	$I_m = \frac{100\%.I}{I_0}$ **(%)**
$GQDs/TiO_2$ NCPs (Cr^{6+}: 0 M)	1095784	100
$GQDs/TiO_2$ NCPs (Cr^{6+}: 0.1 μM)	1022940	93.35
$GQDs/TiO_2$ NCPs (Cr^{6+}: 1.0 μM)	947071	86.43
$GQDs/TiO_2$ NCPs (Cr^{6+}: 500 μM)	913995	83.41
$GQDs/TiO_2$ NCPs (Cr^{6+}: 5 mM)	578877	52.83

$GQDs/TiO_2$ NCPs (Cr^{6+}: 10 mM)	36720	3.35

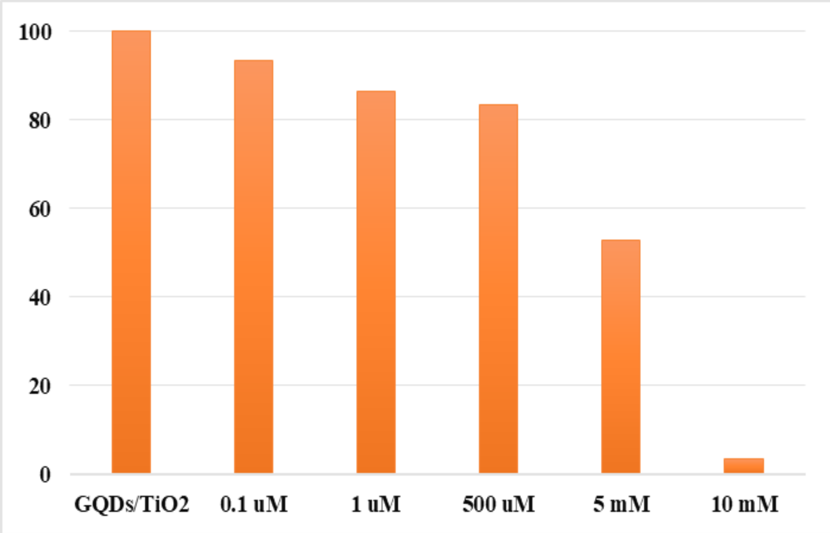

Figure 7. Comparison chart for emission intensity on the PL spectroscopy signal of $GQDs/TiO_2$ nanocomposites samples with various Chromium(VI) concentrations respective: 0 M; 0.1 µM; 1.0 µM; 500 µM; 5 mM; and 10 mM.

IV. Conclusions

Graphene Quantum Dots (GQDs) have been successfully combined with TiO_2 nanoparticles (TiO_2 NPs) for the production of $GQDs/TiO_2$ nanocomposites by green chemistry method (easy to implement, fast reaction time). Besides, the average particle size of $GQDs/TiO_2$ nanocomposites obtained ~10-25 nm, with spherical structure and the composition % of elements present in $GQDs/TiO_2$ nanocomposites corresponds to: C (41.36%); O (54.08%) and Ti (4.56%). Moreover, $GQDs/TiO_2$ nanocomposites were applied to detect for the presence of Chromium(VI) (Cr^{6+}) ions with the extremly low detection concentration with LOD value being ~0.1 µM at an excitation wavelength of 350 nm (UV) and corresponding emission wavelength at 436 nm (visible light). Therefore, it indicated that a sensitive Chromium(VI) ions (heavy metals ions) sensor device could be developed using $GQDs/TiO_2$ nanocomposites material as a photocatalyst material. It can be seen that $GQDs/TiO_2$ nanocomposites are potential and promising materials for applications in fields such as chemical sensors, biosensors, etc, in the current time and in future.

REFERENCES

[1] S. Zhu, J. Zhang, C. Qiao, S. Tang, Y. Li, W. Yuan, B. Li, L. Tian, F. Liu, R. Hu, Strongly green-photoluminescent graphene quantum dots for bioimaging applications, Chemical communications 47(24) (2011) 6858-6860.

[2] M. Zhang, L. Bai, W. Shang, W. Xie, H. Ma, Y. Fu, D. Fang, H. Sun, L. Fan, M. Han, Facile synthesis of water-soluble, highly fluorescent graphene quantum dots as a robust biological label for stem cells, Journal of materials chemistry 22(15) (2012) 7461-7467.

[3] D. Pan, L. Guo, J. Zhang, C. Xi, Q. Xue, H. Huang, J. Li, Z. Zhang, W. Yu, Z. Chen, Cutting sp 2 clusters in graphene sheets into colloidal graphene quantum dots with strong green fluorescence, Journal of Materials Chemistry 22(8) (2012) 3314-3318.

[4] Z.-b. Qu, X. Zhou, L. Gu, R. Lan, D. Sun, D. Yu, G. Shi, Boronic acid functionalized graphene quantum dots as a fluorescent probe for selective and sensitive glucose determination in microdialysate, Chemical Communications 49(84) (2013) 9830-9832.

[5] G. Perini, V. Palmieri, G. Ciasca, M. De Spirito, M. Papi, Unravelling the potential of graphene quantum dots in biomedicine and neuroscience, International Journal of Molecular Sciences 21(10) (2020) 3712.

[6] A. Bratkovsky, Spintronic effects in metallic, semiconductor, metal–oxide and metal–semiconductor heterostructures, Reports on Progress in Physics 71(2) (2008) 026502.

[7] M. Nurunnabi, Z. Khatun, K.M. Huh, S.Y. Park, D.Y. Lee, K.J. Cho, Y.-k. Lee, In vivo biodistribution and toxicology of carboxylated graphene quantum dots, ACS nano 7(8) (2013) 6858-6867.

[8] D. Jiang, Y. Chen, N. Li, W. Li, Z. Wang, J. Zhu, H. Zhang, B. Liu, S. Xu, Synthesis of luminescent graphene quantum dots with high quantum yield and their toxicity study, PLoS One 10(12) (2015) e0144906.

[9] X. Yan, X. Cui, B. Li, L.-s. Li, Large, solution-processable graphene quantum dots as light absorbers for photovoltaics, Nano letters 10(5) (2010) 1869-1873.

[10] L. Wang, Y. Wang, T. Xu, H. Liao, C. Yao, Y. Liu, Z. Li, Z. Chen, D. Pan, L. Sun, Gram-scale synthesis of single-crystalline graphene quantum dots with superior optical properties, Nature communications 5(1) (2014) 1-9.

[11] M. Alexandre, P.J.M.s. Dubois, e.R. Reports, Polymer-layered silicate nanocomposites: preparation, properties and uses of a new class of materials, 28(1-2) (2000) 1-63.

[12] S.S. Ray, M.J.P.i.p.s. Okamoto, Polymer/layered silicate nanocomposites: a review from preparation to processing, 28(11) (2003) 1539-1641.

[13] G. Xie, K. Zhang, B. Guo, Q. Liu, L. Fang, J.R.J.A.m. Gong, Graphene -based mat
hydrogen generation from light -3839. driven water splitting, 25(28) (2013

[14] A.J. Haider, R.H. AL–Anbari, G.R. Kadhim, C.T.J.E.P. Salame, Exploring potential environmental applications of TiO_2 nanoparticles, 119 (2017) 332-345.

[15] S.G. Kumar, L.G.J.T.J.o.p.c.A. Devi, Review on modified TiO_2 photocatalysis under UV/visible light: selected results and related mechanisms on interfacial charge carrier transfer dynamics, 115(46) (2011) 13211-13241.

[16] S. Guo, Z. Wu, W.J.C.S.B. Zhao, TiO_2-based building materials: Above and beyond traditional applications, 54(7) (2009) 1137-1142.

[17] N.R. Monteiro, R.T. Basting, F.L.B.d. AMARAL, F.M.G. França, C.P. Turssi, O.P. Gomes, P.N. Lisboa Filho, K.R. Kantovitz, R.T.J.J.o.A.O.S. Basting, Titanium dioxide nanotubes incorporated into bleaching agents: physicochemical characterization and enamel color change, 28 (2020).

[18] K.Z. Yahya, A.J. Haider, H.S. Tarek, R.M.J.E. Al-Haddad, T. Journal, Effect of substrate temperature on nanostructure titanium dioxide thin films prepared by PLD, 32 (2014).

[19] F.M. Pesci, G. Wang, D.R. Klug, Y. Li, A.J.J.T.J.o.P.C.C. Cowan, Efficient suppression of electron–hole recombination in oxygen-deficient hydrogen-treated TiO_2 nanowires for photoelectrochemical water splitting, 117(48) (2013) 25837-25844.

[20] W.H. Saputera, A.F. Amri, R. Daiyan, D.J.M. Sasongko, Photocatalytic Technology for Palm Oil Mill Effluent (POME) Wastewater Treatment: Current Progress and Future Perspective, 14(11) (2021) 2846.

[21] W. Chen, D. Li, L. Tian, W. Xiang, T. Wang, W. Hu, Y. Hu, S. Chen, J. Chen, Z.J.G.c. Dai, Synthesis of graphene quantum dots from natural polymer starch for cell imaging, 20(19) (2018) 4438-4442.

[22] P.S. Saud, B. Pant, A.-M. Alam, Z.K. Ghouri, M. Park, H.-Y. Kim, Carbon quantum dots anchored TiO2 nanofibers: Effective photocatalyst for waste water treatment, Ceramics International 41(9) (2015) 11953-11959.

[23] X. Hao, Z. Jin, J. Xu, S. Min, G. Lu, Functionalization of TiO_2 with graphene quantum dots for efficient photocatalytic hydrogen evolution, Superlattices and Microstructures 94 (2016) 237-244.

[24] N.-Q. Ou, H.-J. Li, B.-W. Lyu, B.-J. Gui, X. Sun, D.-J. Qian, Y. Jia, X. Wang, J. Yang, Facet-dependent interfacial charge transfer in TiO_2/nitrogen-doped graphene quantum dots heterojunctions for visible-light driven photocatalysis, Catalysts 9(4) (2019) 345.

[25] E. Mahdi, M.H. Abdul Shukor, M.S. Meor Yusoff, P. Wilfred, XRD and EDXRF analysis of anatase nano-TiO_2 synthesized from mineral precursors, Advanced Materials Research, Trans Tech Publ, 2013, pp. 179-185.

[26] H. Xie, C. Hou, H. Wang, Q. Zhang, Y. Li, S, N co-doped graphene quantum dot/TiO_2 composites for efficient photocatalytic hydrogen generation, Nanoscale research letters 12(1) (2017) 1-8.